Shaft Sensor-less FOC Control of an Induction Motor Using Neural Estimators

Peter Girovský, Jaroslav Timko, Jaroslava Žilková

Department of Electrical Engineering and Mechatronics, Technical University of Košice, Letná 9, 042 00 Košice, Slovak Republic
peter.girovsky@tuke.sk, jaroslav.timko@tuke.sk, jaroslava.zilkova@tuke.sk

Abstract: The paper deals with a shaft sensor-less field oriented control structure for an induction motor based on neural network estimators. The first part presents the theoretical knowledge. The second part presents the simulation and results of designing neural estimators for observing the magnetic flux and the motor angular speed for induction motor field oriented control in MATLAB-Simulink. Controllers for simulation of shaft sensor-less field oriented control have been designed by state space method. An achieved simulation result of the neural angular speed estimator has been verified by system of AC converter – induction motor by Real-Time system.

Keywords: induction motor; neural network; sensor-less control; vector control

1 Introduction

Motors play important roles in industrial production and in many other applications. In their early days, DC motors had the advantage of precise speed control when utilized for the purpose of accurate driving. However, DC motors have the disadvantage of brush erosion, maintenance requirements, environmental effects, complex structures and power limits. On the other hand, induction motors are robust, small in size, low in cost, and almost maintenance-free.

Hasse [9] and Blaschke [10] developed a field oriented control theory to simplify the structure of IM speed control used to drive the DC motor. In recent years, the field oriented control theory has become more feasible due to progress in the development of electronics techniques and high-speed microprocessors. Nonlinear control problems can often be solved if full state information is available; in the IM case, the rotor states are immeasurable and often it is too costly to monitor the angular speed of the rotor.

In most applications, speed sensors are necessary in the speed control loop. On the other hand, there are applications where lower performance is required, cost reduction and high reliability are necessary, or a hostile environment does not

allow for using speed sensors. In these fields, speed sensor-less IM control can be usefully applied. Many different solutions for the estimation of states variables or model parameters have been proposed recently, for example, estimators utilizing motor construction properties, estimators based on the drive dynamic model or estimators based on artificial intelligence [7, 8, 13, 15, 16].

Sensor-less controllers have been proposed which depend on adaptive control and observer theory, on optimal observer design by applying Kalman filter theory [11, 12], on sliding mode control [2, 3], and on using artificial intelligence methods [1, 4, 5, 6, 14].

At present, requirements on the dynamic precision are not too strict and virtual or soft sensors are alternatively successfully utilized. Estimators based on artificial intelligence are divided into the following groups:

- systems based on the fuzzy logic,

- systems based on neural networks,

- systems based on hybrid systems,

- systems based on evolutionary algorithms (genetic algorithms).

2 Simulation Design of a Neural Estimator for Field Oriented Control of Induction Motor

The neural modelling can perform estimation of the induction motor angular speed or of other non-measurable variables on the neural networks base.

Nowadays, there are field oriented controlled drives based on different solutions and performances which are commonly used in industry. With field-oriented techniques, the decoupling of flux and torque control commands of the IM is guaranteed, and the induction motor can be controlled linearly, like a separately excited DC motor. The DC motor like performance can be obtained by preserving a fixed and orthogonal orientation between the field and armature fields in the induction motor by orientation of the stator current with respect to the rotor flux in order to attain independently controlled flux and torque. Using the field oriented control principle, the stator current component i_{d1} is aligned in the direction of the rotor flux vector and the stator current component i_{q1} is aligned in the direction perpendicular to it. The rotor flux orientation in the squirrel-cage rotor IM cannot be directly measured, but it can be obtained from terminal variables.

After using transformation of coordinates *d*, *q* to the rotating system *x-y*, the electric torque is proportional to the i_{1y} component and the relation between the rotor flux and i_{1x} component is given by the first order linear transfer function with $T_2 = L_2/R_2$ time constant.

From this fact and for the considered flux control, the stator current and voltage components were chosen as input signals for the reconstruction of the induction motor speed. The developed estimators were trained according to selected training patterns from the direct field oriented control of the induction motor. Block diagram of the control scheme is presented in Figure 1.
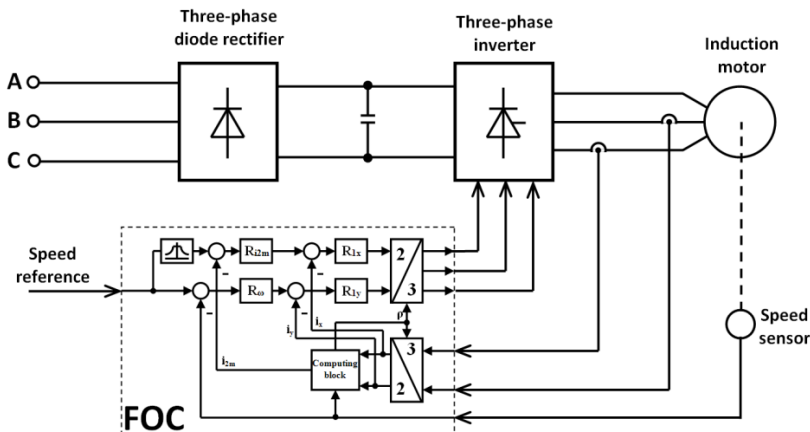

Figure 1

Basic field oriented control scheme

2.1 Induction Motor FOC Simulation Design

Field oriented control simulation design had been made for induction motor with the following parameters: P_n=0,75 kW; U_n= 220V/380V; I_n= 3,8 A/2,2 A; n_n= 1380 rpm; p=2; s=0,08; J=5,4.10^{-3} kgm^2

In the design of state control by method of the poles determine for two input variables and one output based on the following equations:

$$\sigma T_1 \frac{di_{1x}}{dt} + i_{1x} = \frac{K_T u_{1x}}{R_1} - (1-\sigma)T_1 \frac{di_{2m}}{dt} + \sigma T_1 \omega_{2m} i_{1y} \tag{1}$$

$$\sigma T_1 \frac{di_{1y}}{dt} + i_{1y} = \frac{K_T u_{1y}}{R_1} - (1-\sigma)T_1 \omega_{2m} i_{2m} - \sigma T_1 \omega_{2m} i_{1x} \tag{2}$$

$$T_2 \frac{di_{2m}}{dt} + i_{2m} = i_{1x} \tag{3}$$

$$\frac{i_{1y}}{T_2 i_{2m}} + \omega = \omega_{2m} \tag{4}$$

$$\frac{J}{p} \frac{d\omega}{dt} = \frac{3p}{2} \frac{L_h}{1+\sigma_2} i_{2m} i_{1y} - m_z \tag{5}$$

Define the state variables: $i_{2m}=x_1$; $i_{1x}=x_2$; $\omega=x_3$; $i_{1y}=x_4$; $m_z=z$; $u_1=u_{1x}/K_T$; $u_2=u_{1y}/K_T$

Then, written can be the state equation for induction motor:

$$\dot{\underline{x}} = \begin{bmatrix} -a_1x_1 + a_1x_2 \\ f_2(\underline{x}) \\ a_3x_1x_4 \\ f_4(\underline{x}) \end{bmatrix} + \begin{bmatrix} 0 & 0 \\ b & 0 \\ 0 & 0 \\ 0 & b \end{bmatrix}.\underline{u} + \begin{bmatrix} 0 \\ 0 \\ -e \\ 0 \end{bmatrix}.z = a(x) + B.u + e.z$$

(6)

$$y = x_3 = c(x)$$

The constants and functions used in the state equation (6):

$$a_1 = \frac{1}{T_2}; \quad a_2 = \frac{1}{\sigma T_1}; \quad a_3 = \frac{3p^2}{2J}\frac{L_h}{1+\sigma_2}; \quad a_4 = \frac{1-\sigma}{\sigma}; \quad \sigma_2 = \frac{L_{2\sigma}}{L_h}; \quad \sigma = 1 - \frac{L_h^2}{L_1.L_2};$$

$$b = \frac{K_T}{\sigma L_1}; \quad e = \frac{p}{J}$$

$$f_2(\underline{x}) = a_1.a_4.x_1 - (a_2 + a_1.a_4)x_2 + x_3.x_4 + a_1.\frac{x_4^2}{x_1}$$

$$f_4(\underline{x}) = -(a_2 + a_1.a_3)x_4 - a_4.x_1.x_3 - x_2.x_3 - a_1.\frac{x_2.x_4}{x_1}$$

Nonlinear function $f_2(x), f_4(x)$ in the control scheme shown in Fig. 2 compensating for introduction of control u, so as to simplify the state equation:

$$u = \frac{1}{b}\begin{bmatrix} -f_2(x) + v_2 - r.x_2 \\ -f_4(x) + v_4 - r.x_4 \end{bmatrix}$$

$$\dot{\underline{x}} = \begin{bmatrix} -a_1 & a_1 & 0 & 0 \\ 0 & -r_2 & 0 & 0 \\ 0 & 0 & 0 & a_3 \\ 0 & 0 & 0 & -r_4 \end{bmatrix}.\underline{x} + \begin{bmatrix} 0 & 0 \\ 1 & 0 \\ 0 & 0 \\ 0 & 1 \end{bmatrix}\begin{bmatrix} v_2 \\ v_4 \end{bmatrix}$$

2.1.1　Current Sub-Circuit (R_{1x}, R_{1y})

$$\begin{bmatrix} \dot{x}_2 \\ \dot{v}_2 \end{bmatrix} = \begin{bmatrix} -r_2 & 1 \\ -K_2 & 0 \end{bmatrix}\begin{bmatrix} x_2 \\ v_2 \end{bmatrix} + \begin{bmatrix} 0 \\ K_2 \end{bmatrix}.w_2$$

$$v_2 = k_2\int(w_2 - x_2)dt; \quad \dot{v}_2 = K_2.(w_2 - x_2)$$

The characteristic polynomial of system $P_{(\lambda)}$:

$$P_{(\lambda)} = \det(\lambda.\underline{I} - \underline{A}) = \det\begin{bmatrix} \lambda + r_2 & -1 \\ K_2 & \lambda \end{bmatrix} = \lambda^2 + r_2.\lambda + K_2$$

For current controller select the damping $d=0.85$, regulation time $t_r=0.05s$ and determine the desired characteristic polynomial $P_{(s)}$:

$$P_{(s)} = s^2 + 146.s + 7354$$

By comparing the characteristic polynomial and the desired characteristic polynomial we obtain controller constants K_2, K_4 and r_2, r_4 where $K_2 = K_4$ and $r_2 = r_4$.

2.1.2　Superior Circuit of Magnetizing Current (R_{i2m})

$$\begin{bmatrix} \dot{x}_1 \\ \dot{x}_2 \\ \dot{v}_2 \\ \dot{v}_1 \end{bmatrix} = \begin{bmatrix} -a_1 & a_1 & 0 & 0 \\ 0 & -r_{12} & 1 & 0 \\ -K_2.r_{11} & -K_2(1+r_{12}) & -K_2.d_{12} & K_2 \\ -K_1 & 0 & 0 & 0 \end{bmatrix}\begin{bmatrix} x_1 \\ x_2 \\ v_2 \\ v_1 \end{bmatrix} + \begin{bmatrix} 0 \\ 0 \\ 0 \\ K_2 \end{bmatrix}.w_1$$

$$w_2 = v_1 - r_{11}.x_1 - r_{12}.x_2 - d_{12}.v_2 \; ; \; \dot{v}_1 = K_1.(w_1 - x_1)$$

The characteristic polynomial of system $P_{(\lambda)}$:

$$P_{(\lambda)} = \det(\lambda.\underline{I} - \underline{A}) = \lambda^4 + \lambda^3(a_1 + r_{12} + K_2.d_{12}) + \lambda^2(a_1.r_{12} + a_1.K_2.d_{12} + K_2 + K_2.r_{12}) +$$

$$+ \lambda.K_2.a_1.(r_2.d_{12} + 1 + r_{12} + r_{11}) + a_1.K_1.K_2$$

Select the damping $d=0.85$, regulation time $t_r=0.1s$ and determine the desired characteristic polynomial $P_{(s)}$:

$$P_{(s)} = s^4 + 214.s^3 + 1793s^2 + 162020.s + 9079700$$

By comparing of the characteristic polynomial and the desired characteristic polynomial we obtain controller constants K_1, r_{11}, r_{12}, d_{12}.

2.1.3　Superior Circuit of Speed (R_ω)

$$\begin{bmatrix} \dot{x}_3 \\ \dot{x}_4 \\ \dot{v}_4 \\ \dot{v}_3 \end{bmatrix} = \begin{bmatrix} 0 & 0 & a_3 & 0 \\ 0 & 0 & 1 & -r_4 \\ -K_4.r_{33} & -K_4(1+r_{34}) & -K_3.d_{34} & K_4 \\ -K_3 & 0 & 0 & 0 \end{bmatrix}.\begin{bmatrix} x_3 \\ x_4 \\ v_4 \\ v_3 \end{bmatrix} + \begin{bmatrix} 0 \\ 0 \\ 0 \\ K_3 \end{bmatrix}.w_3$$

$$w_4 = v_3 - r_{33}.x_3 - r_{34}.x_4 - d_{34}.v_4 \; ; \; \dot{v_3} = K_3.(w_3 - x_3)$$

The characteristic polynomial of system $P_{(\lambda)}$:

$$P_{(\lambda)} = \det(\lambda.\underline{I} - \underline{A}) = \lambda^4 + \lambda^3 (r_{34} + K_4.d_{34}) + \lambda^2.K_4 (r_4.d_{34} + 1 + r_{34}) + \lambda.(a_3.K_4.r_{33}) + a_3.K_3.K_4$$

Select the damping $d=0.85$, regulation time $t_r=0.1s$ and determine the desired characteristic polynomial $P_{(s)}$:

$$P_{(s)} = s^4 + 214.s^3 + 1793s^2 + 162020.s + 9079700$$

By comparing of the characteristic polynomial and the desired characteristic polynomial obtained are controller constants K_3, r_{33}, r_{34}, d_{34}.

Constants calculated for all circuits of controller are used by the field oriented control scheme shown in Figure 2.
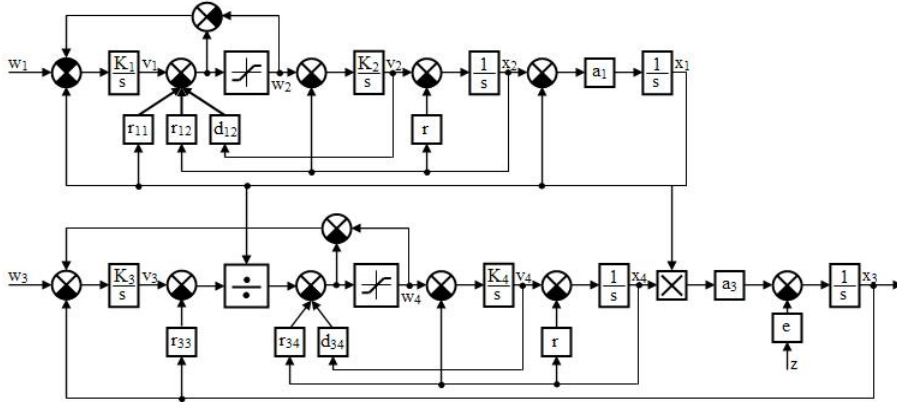

Figure 2
Simulation field oriented control scheme

2.2   Magnetising Current Neural Estimator

If for vector control the *x*-th component of the stator current vector is considered as a basis of current-creating component, then the magnetising current i_{2m} estimator will process current-creating component of the stator current.

As mentioned above, the magnetising current i_{2m} neural estimator bases its estimation of the current-creating component of stator current i_{1x}. Dependence between currents i_{2m} and i_{1x} is linear, and hence the estimator can be made up of a feed-forward neural network without any hidden layer. For the activating function, the *purelin* linear function can be used. The input data vector consists of values of the stator current i_{1x} in step *(k)* and step *(k-1)*, respectively, and also the preceding value of magnetising current i_{2m} in step *(k-1)*. A basic diagram of such neural estimator is shown in Figure 3.
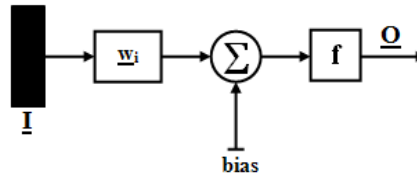
Figure 3

Basic diagram of magnetising current i_{2m} neural estimator

Here, $\underline{O}$ stands for output values vector, $\underline{I}$ is the input data vector, and w_i presents weights of individual connections of neurons.

$$\underline{O} = f\left[\sum \underline{I}.\underline{w}_i + bias\right] \tag{7}$$

Substituting the input matrix to equation (7), we will obtain the equation for the magnetising current neural estimator in the following form:

$$i_{2m}(k) = purelin\left(\begin{bmatrix} i_{1x}(k) \\ i_{1x}(k-1) \\ i_{2m}(k-1) \end{bmatrix}\underline{w}_i + bias\right) \tag{8}$$

where current $i_{2m}(k)$ is the output variable and the input variables are $i_{1x}(k)$, $i_{1x}(k-1)$ and $i_{2m}(k-1)$.

2.3   Speed Neural Estimator

If for the basis of torque-creating component we establish the *y*-th component of the vector, then the speed estimator will estimate this torque creating component from the stator voltage and current.

As was already mentioned above, the angular speed ω neural estimator bases its estimation on the torque component of stator voltage u_{1y} and current i_{1y}. The relation between the input and output quantities is not represented by a simple linear dependency, and this is the reason why for the estimation a cascade neural network with one hidden layer consisted of eight neurons will be used. As an activating function for the hidden layer used, there was the *tansig* nonlinear function and for the output layer used was a *purelin* linear function. The input data vector is represented by values of stator voltage u_{1y} and stator current i_{1y} in steps *(k)* and *(k-1)*, as well as by value of magnetising current i_{2m} in steps *(k)* and *(k-1)*. Basic diagram of such a neural estimator is shown in Figure 4.
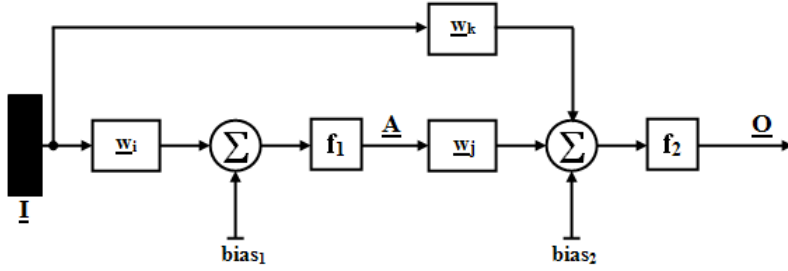
Figure 4

Basic diagram of ω motor angular speed neural estimator

In the figure, $\underline{O}$ is the output values vector, $\underline{I}$ presents a vector of input variables and w_i, w_j, w_k are weights of individual connections of neurons.

$$\underline{A} = f_1\left[\sum \underline{I}.\underline{w}_i + bias_1\right]$$

$$\underline{O} = f_2\left[\sum\left(\underline{A}.\underline{w}_j + \underline{I}.\underline{w}_k\right) + bias_2\right]$$

(9)

Post substituting the input matrix to equation (9) the neural speed estimator can be described by the following equation:

$$\omega(k) = purelin\left(\begin{bmatrix} u_{1y}(k) \\ u_{1y}(k-1) \\ i_{1y}(k) \\ i_{1y}(k-1) \\ i_{2m}(k) \\ i_{2m}(k-1) \end{bmatrix}\underline{w}_j + tansig\left(\begin{bmatrix} u_{1y}(k) \\ u_{1y}(k-1) \\ i_{1y}(k) \\ i_{1y}(k-1) \\ i_{2m}(k) \\ i_{2m}(k-1) \end{bmatrix}\underline{w}_i + bias1\right)\underline{w}_k + bias2\right)$$

(10)

where the output quantity is *ω(k)* angular speed value and where the input are values *$u_{1y}(k)$, $u_{1y}(k-1)$, $i_{1y}(k)$, $i_{1y}(k-1)$, $i_{2m}(k)$* and *$i_{2m}(k-1)$*.

3   Simulation Results

In the following, we show the simulation results of sensor-less vector control of an induction motor when applying neural estimators of the speed and magnetising current, respectively.

The principal diagram of the vector control with connected neural estimators of the magnetising current and speed is shown in Figure 5.
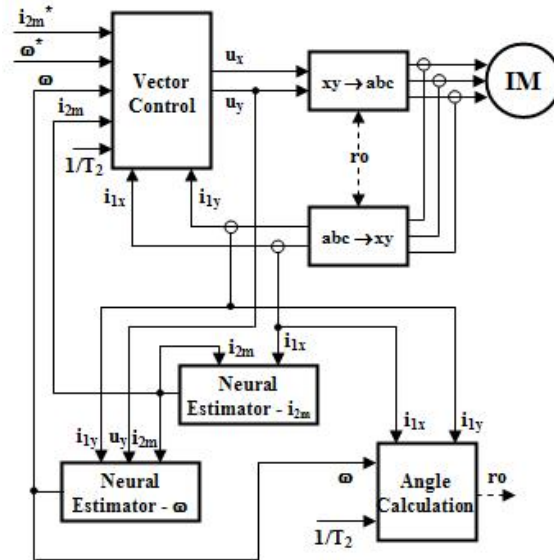
Figure 5

Basic diagram of vector control with neural estimators

Simulation, design and training of neural estimators were performed for the induction motor with parameters: P_n=0,75 kW; U_n= 220V/380V; I_n= 3,8 A/2,2 A; n_n= 1380 rpm; p=2; s=0,08; J=5,4.10^{-3} kgm^2
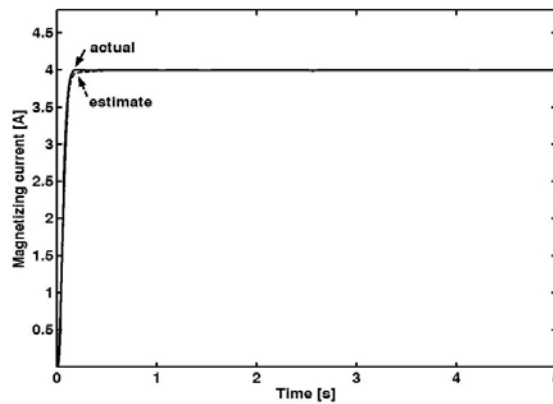

Figure 6

Comparison of the estimated versus actual magnetising current

Figures 6 and 7 show a comparison of real and observed values of the magnetizing current and the angular speed. A dashed line shows there is the required angular speed value during starting, reversing and loading transients. In time of 2s the motor was loaded by the rated load torque.
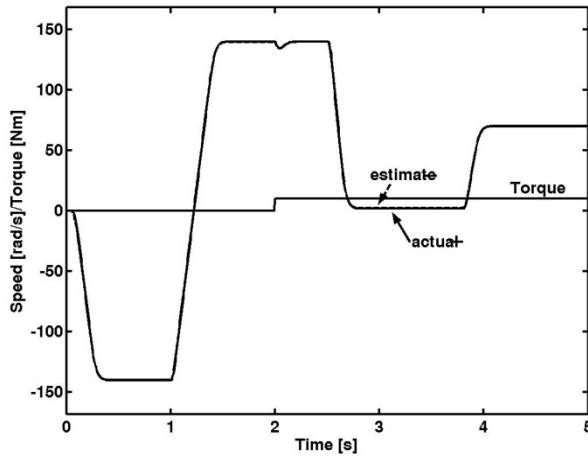
Figure 7
Comparison of the estimated versus actual speed of the IM

The waveforms shown in Figures 6 and 7 are valid for the case of no feedback to control from the neural observers but led directly from the motor mathematical model.
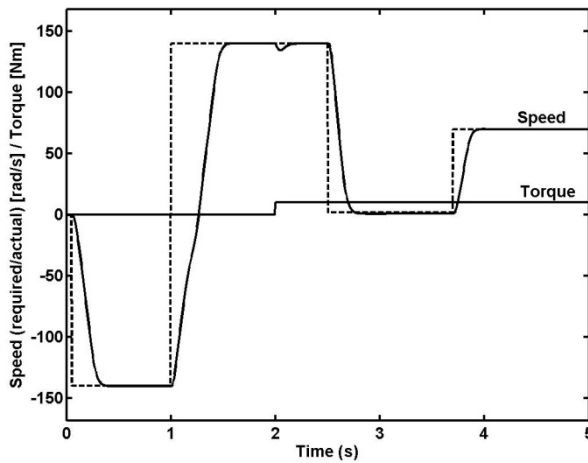

Figure 8
Transients of desired versus real angular speed and the motor load torque

Shown in Figure 8 is a simulated response of the induction motor angular speed (in solid line) at conditions identical with the previous one, shown in Figure 7. In this case, and the same as in any following ones, the feedback to control was introduced from neural observers of the magnetising current and angular speed.

3.1 Experimental Verification

For verification of simulation results, an experimental Real-Time system based on RT-LAB system was used. The principal scheme of the whole system is show in Figure 9.

The experimental system consists of the SIMOVERT MASTERDRIVES Vector Control and an induction motor with the same parameters as those of the motor used for simulation. Used as the load there was a dynamo with resistor and the base of this experimental system consists of Real-time system with NI PCI-6025E.
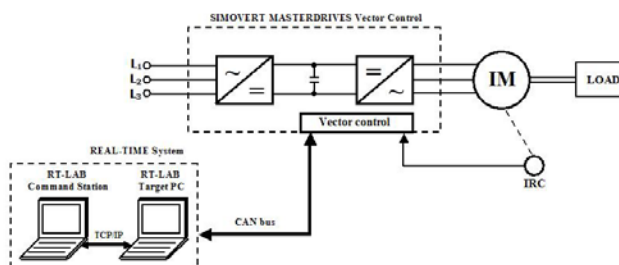

Figure 9

Principal scheme of Real-Time system

3.2 Neural Estimation for Experimental Verification

Regarding different ways of vector control in SIMOVERT MASTERDRIVES, a Vector Control (system in rotary coordinates *d-q*), used for design of speed neural estimator, was the input stator voltage in step *(k)* – $u(k)$, in the step *(k-1)* - $u(k-1)$ and value of current components *d,q* in step (k) – $i_d(k)$, $i_q(k)$ and in step *(k-1)* - $i_d(k-1)$, $i_q(k-1)$. For off-line training using the Levenberg-Marquardt algorithm 126013 samples in aggregate were used. The output vector for training is represented by value of the rotor speed $\hat{o}(k)$ in step *(k)*.

For the speed neural estimator we used a cascade neural network with one hidden layer having six input neurons and six hidden neurons. For the hidden layer activating function used was the *tansig* nonlinear function and for the output layer we used *purelin* linear function. Using them we obtained an equation for neural estimator of speed in the following form:

$$\hat{o}(k) = purelin\left(\begin{bmatrix} u(k) \\ u(k-1) \\ i_d(k) \\ i_d(k-1) \\ i_q(k) \\ i_q(k-1) \end{bmatrix}\underline{w}_j + \boldsymbol{tansig}\left(\begin{bmatrix} u(k) \\ u(k-1) \\ i_d(k) \\ i_d(k-1) \\ i_q(k) \\ i_q(k-1) \end{bmatrix}\underline{w}_i + bias1\right)\underline{w}_k + bias2\right) \tag{11}$$

4 Experimental Results

Presented in the following are the simulation results of sensor-less vector control of an induction motor when using neural estimators of speed. The principal diagram of vector control effected with the use of neural estimator of speed is shown in Figure 10.
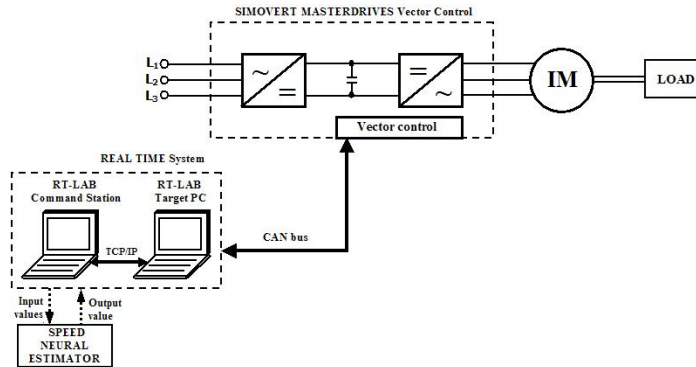

Figure 10

Principal scheme of Real-Time system with neural estimator

a) speed

b) voltage
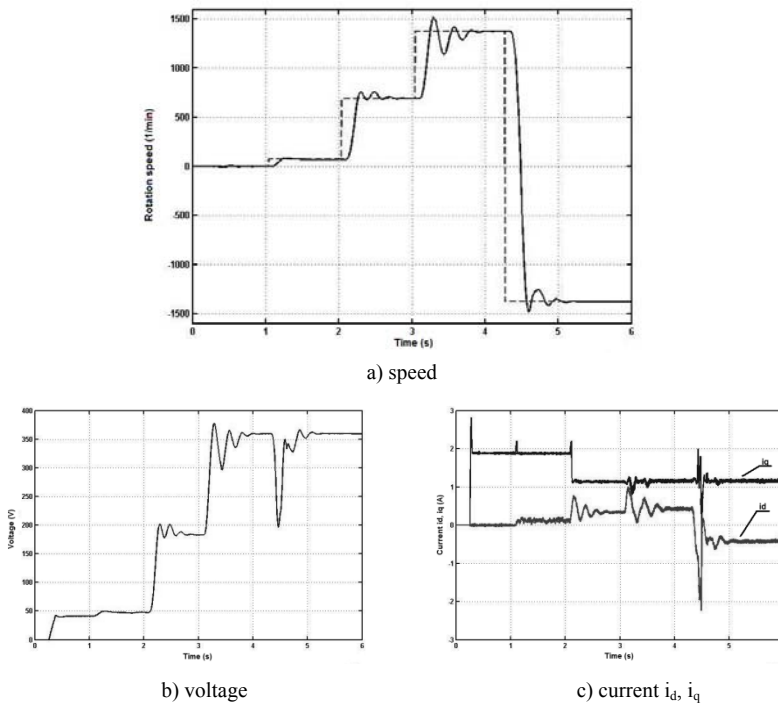

c) current i_d, i_q

Figure 11

Time courses of desired versus actual rotor speed without load and relevant voltage and current

In Figures 11 and 12 are shown courses of desired (dash line) and actual rotor speeds of induction motor in the vector control using the scheme according to Figure 10.

At time 1 second, the required value of rotor speed changed from 0% to 5% of nominal speed, at time 2 seconds, from 5% to 50%; at time 3 seconds, from 50% to 100% of nominal rotor speed and at time 4 seconds, the induction motor reversed.

For verification we used an experimental real time system. The results obtained, illustrated by respective waveforms, validate the possibility of utilising artificial neural networks in sensor-less vector control of the induction motor. The drive features better adaptability and robustness in comparison with a drive without estimator.
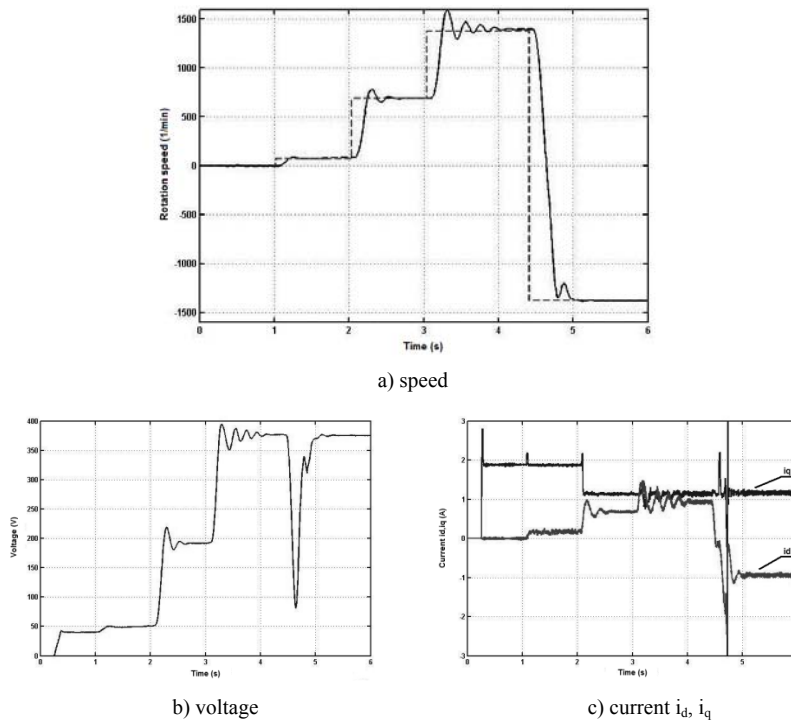
a) speed

b) voltage   c) current i_d, i_q

Figure 12

Time courses of desired versus actual rotor speed with load and relevant voltage and current

Conclusions

The paper is concerned with designing induction motor neural estimators. Based on easily measurable quantities, such as components of stator current and voltage, we designed estimators of the motor speed and magnetising current, utilizing feed-forward and cascade neural networks. Both these networks were trained off-line

using the Levenberg-Marquardt algorithm, which is a modification of the traditional back-propagation training algorithm.

The results arrived at, illustrated by respective waveforms, validate the possibility of utilising artificial neural networks in the sensor-less vector controlling of an induction motor, while also taking advantage of their advantageous properties, such as adaptability and robustness.

At the end of this paper presented are research results. For applied verification used was experimental Real-Time system.

Acknowledgement

References

[1]　Vas P., "Artificial-Intelligence-based Electrical Machines and Drives", Oxford University Press, Oxford, 1999

[2]　Vittek J., Dodds S. J., Makyš P., Lehocký P., "An Observer Design for Forced Dynamics Control of AC Drives", Transcom 2007, Žilina, Slovensko, pp. 207-210, 2007

[3]　Vittek J., Bris P., Štulrajter M., Pácha M., "Chattering Free Sliding Mode Control Law for Position Control of the Drive Employing Induction Motor", Power Engineering Conference 2008, AUPEC '08, Australasian Universities, pp. 1-6, 14-17 Dec., 2008

[4]　Kuchar M., Brandštetter P., Kaduch M., "Sensor-less Induction Motor Drive with Neural Network". IEEE, Annu. Power Elec. Specialists Conf.m pp. 3301-3305, 2004

[5]　Jovankovič J., Žalman M., "Application of the Virtual Sensors Based on the Artificial Neural Networks", EDPE'03, International conference, Slovakia, 2003, pp. 486-490

[6]　Bensalem Y., Abboud W., Sbita L., Abdelkrim M. N., "A Sensor-less Neural Network Speed Control of Induction Motor Drive", Int. Journal of Signal System Control and Engineering Application 1 (2): pp. 150-158, 2008

[7]　Jadlovská A., Kabakov N., Sarnovský J., "Predictive Control Design Based on Neural Model of a Non-linear System", Acta Polytechnica Hungarica, Vol. 5, No. 4, pp. 93-108, 2008

[8]　Jamuna V., Reddy S. R., "Modeling and Speed Control of Induction Motor Drives Using Neural Network", Annals of Diarea de Jos University of Galati, III, Vol. 33, No. 1, pp. 40-49, 2010

[9]   Hasse K., "Zur Dynamik Drehzahlgeregelter Antriebe mit stromrichtergespeisten Asynchron-kurschlusslaüfer Maschinen", Techn. Hochsch: Darmstadt, Dissertation, 1969, pp. 74-78

[10]   Blaschke F., "The Principle of Field Orientation as Applied to the New Transvektor Closed–Loop Control System for Rotating-Field Machines", Siemens Rev. 39 (5): 1972, pp. 217-220

[11]   Meziane S., Toufouti R., Benalla H., "Nonlinear Control of Induction Machines Using an Extended Kalman Filter", Acta Polytechnica Hungarica, Vol. 5, No. 4, pp. 41-58, 2008

[12]   Žilková J., Timko J., Berko J., "Speed Sensor-less Control of an Induction Motor Drive Using Extended Kalman Filter", In: Acta Technica ČSAV 50, No. 4, Prague, 2005, pp. 279-289

[13]   Timko J., Žilková J., Balara D., "Artificial Neural Networks Application in Electrical Drives", (in Slovak), Calypso s.r.o., Košice, 2002, p. 239, ISBN 80-85723-27-1

[14]   Timko J., Žilková J., Girovský P., "Shaft Sensor-less Vector Control of an Induction Motor", In: Acta Technica CSAV, Vol. 52, No. 1 (2007), pp. 81-91, ISSN 0001-7043

[15]   Timko J., Žilková J., Girovský P., "Modeling and Control of Electrical Drives Using Neural Networks", (in Slovak), C-Press, Košice, 2009, p. 202, ISBN 978-80-8086-124-7

[16]   Žilková J., Timko J., Girovský P., "Nonlinear System Control Using Neural Networks", Acta Polytechnica Hungarica, Vol. 3, No. 4, pp. 85-94, 2006